Baghdad Science Journal

Volume 23 | Issue 1 Article 10

1-1-2026

Porosity and Structural Integrity of Tin-Polydimethylsiloxane (PDMS) Composites for Radiation Shielding Application

Hanisah Zainal Abidin
Department of Applied Sciences, Universiti Teknologi MARA Cawangan Pulau Pinang, 13500 Permatang Pauh, Pulau Pinang, Malaysia, 2023650308@student.uitm.edu.my

Nur Maizatul Azra Mukhtar
Department of Applied Sciences, Universiti Teknologi MARA Cawangan Pulau Pinang, 13500 Permatang Pauh, Pulau Pinang, Malaysia AND Faculty of Health Sciences, Universiti Teknologi MARA Cawangan Pulau Pinang, 13200 Kepala Batas, Pulau Pinang, Malaysia; AND Department of Biomedical Imaging, Advanced Medical and Dental Institute, Universiti Sains Malaysia, SAINS@BERTAM, 13200 Kepala Batas, Pulau Pinang, Malaysia, nurmaizatul038@uitm.edu.my

Ainorkhilah Mahmood
Department of Applied Sciences, Universiti Teknologi MARA Cawangan Pulau Pinang, 13500 Permatang Pauh, Pulau Pinang, Malaysia, ainorkhilah_sp@uitm.edu.my

Nor Aimi Abdul Wahab
Department of Applied Sciences, Universiti Teknologi MARA Cawangan Pulau Pinang, 13500 Permatang Pauh, Pulau Pinang, Malaysia, noraimi108@uitm.edu.my

Rafidah Zainon
Department of Biomedical Imaging, Advanced Medical and Dental Institute, Universiti Sains Malaysia, SAINS@BERTAM, 13200 Kepala Batas, Pulau Pinang, Malaysia, rafidahzainon@usm.my

How to Cite this Article
See next page for additional authors
Abidin, Hanisah Zainal; Mukhtar, Nur Maizatul Azra; Mahmood, Ainorkhilah; Wahab, Nor Aimi Abdul; Zainon, Rafidah; Roslan, Nurul Syafiqah; Izaham, Nur Iwani Nor; and Shah, Aishah Zarzali (2026) "Porosity and Structural Integrity of Tin-Polydimethylsiloxane (PDMS) Composites for Radiation Shielding Application," *Baghdad Science Journal*: Vol. 23: Iss. 1, Article 10.
DOI: https://doi.org/10.21123/2411-7986.5143

Porosity and Structural Integrity of Tin-Polydimethylsiloxane (PDMS) Composites for Radiation Shielding Application

Authors

Hanisah Zainal Abidin, Nur Maizatul Azra Mukhtar, Ainorkhilah Mahmood, Nor Aimi Abdul Wahab, Rafidah Zainon, Nurul Syafiqah Roslan, Nur Iwani Nor Izaham, and Aishah Zarzali Shah

BAGHDAD SCIENCE JOURNAL 2026;23(1):121–137

Scan the QR to view the full-text article on the journal website

SPECIAL ISSUE ARTICLE

Porosity and Structural Integrity of Tin-Polydimethylsiloxane (PDMS) Composites for Radiation Shielding Application

Hanisah Zainal Abidin [1], Nur Maizatul Azra Mukhtar [1,2,3,*], Ainorkhilah Mahmood [1], Nor Aimi Abdul Wahab [1], Rafidah Zainon [3], Nurul Syafiqah Roslan [1], Nur Iwani Nor Izaham [4], Aishah Zarzali Shah [5]

[1] Department of Applied Sciences, Universiti Teknologi MARA Cawangan Pulau Pinang, 13500 Permatang Pauh, Pulau Pinang, Malaysia
[2] Faculty of Health Sciences, Universiti Teknologi MARA Cawangan Pulau Pinang, 13200 Kepala Batas, Pulau Pinang, Malaysia
[3] Department of Biomedical Imaging, Advanced Medical and Dental Institute, Universiti Sains Malaysia, SAINS@BERTAM, 13200 Kepala Batas, Pulau Pinang, Malaysia
[4] Faculty of Applied Sciences, Universiti Teknologi MARA, 40450 Shah Alam, Selangor, Malaysia
[5] Centre of Foundation Studies UiTM, Universiti Teknologi MARA Cawangan Selangor, Kampus Dengkil, 43800 Dengkil, Selangor, Malaysia

ABSTRACT

Ionizing radiation benefits medical treatments and diagnostics. However, it also poses significant health risks, such as from the scattering radiation and unintended exposure. Lead is a common shielding material used for its excellent gamma ray attenuation performance, but it presents ergonomic and environmental challenges. This study assesses the structural and potential radiation absorption properties of the tin-polydimethylsiloxane (PDMS) composites. The composites were fabricated with different metal concentrations and tested for radiation protection efficiency (RPE), structural characteristics, chemical structure, and porosity. Gamma-ray spectroscopy was used to characterize radiation, with Cd-109 as a primary source. Pure tin/PDMS (PT) had the highest RPE compared to copper-tin alloy/PDMS (TA) and copper-tin alloy-pure tin/PDMS (PA), owing to its high atomic number and low porosity. Structural and chemical investigations, including FESEM and FTIR analysis, validated the composites' homogeneity and chemical bonding. The porosity of the composite is evaluated using ImageJ analysis. The results highlight that each composite's porosity increase as the composition of metal filler increases. However, radiation attenuation capabilities more affected by the atomic number of the metal used and metal filler compositions within the composites. Porosity analysis revealed that PT had the lowest porosity among the composites, which may contribute to its superior shielding efficiency. Conversely, TA and PA showed lower atomic number and higher porosity, which disrupted their structural integrity and may reduce photon attenuation. Therefore, methods such as hot pressure, degassing, or vacuum procedures are suggested to reduce the porosity and enhance the radiation shielding within the composites.

Keywords: Composites, Metal, Polymer, Porosity, Radiation shielding

Introduction

Radiation is described as the energy that can travel through matter and space. Various industries widely use ionizing radiation sources like X-rays and gamma rays.[1] Exposure to the high energy of this ionizing radiation may negatively impact humans.[2] Therefore, effective shielding materials are necessary to protect workers from the hazards of ionizing radiation. While ionizing radiation has beneficial applications, such as

Received 28 February 2025; revised 19 July 2025; accepted 22 July 2025.
Available online 1 January 2026

* Corresponding author.
E-mail addresses: 2023650308@student.uitm.edu.my (H. Zainal Abidin), nurmaizatul038@uitm.edu.my (N. Maizatul Azra Mukhtar), ainorkhilah_sp@uitm.edu.my (A. Mahmood), noraimi108@uitm.edu.my (N. Aimi Abdul Wahab), rafidahzainon@usm.my (R. Zainon), rafidahzainon@usm.my (N. Syafiqah Roslan), 2024592857@student.uitm.edu.my (N. Iwani Nor Izaham), aishah.zarzali@uitm.edu.my (A. Zarzali Shah).

International Conference on Discoveries in Applied Sciences and Applied Technology (DASAT2025)
https://doi.org/10.21123/2411-7986.5143

in cancer treatment through radiation therapy, it is also associated with negative health impacts. These include oxidative stress, increased cancer risk, organ damage, and other adverse effects, particularly with prolonged exposure. Consequently, it is crucial to implement safety measures, including exposure control and regular monitoring, to protect healthcare workers from these risks.[1–4]

Lead is known for its high density ($\rho = 11.34$ g cm^{-3}), low cost, and strong absorption properties, making it highly effective as a material for attenuating radiation. It is widely used in medical industries to reduce the energy of radiation and block one from radiation exposure.[5] However, using lead-based protective equipment has drawbacks, such as high toxicity, low mechanical properties (inflexibility), low chemical stability and heaviness that lead to ergonomic issues.[1] For example, workers often report back pain from the weight of lead aprons after extended wear. Additionally, lead is environmentally hazardous; the high cost of lead disposal and improper disposal can release toxic chemicals harmful to human health. Due to these concerns, recent studies have focused on finding alternative metals for radiation shielding or developing new materials for personal protective equipment (PPE).[6–9]

Although lead is commonly used for radiation shielding, metal alone poses weight challenges, particularly the heavy burden it places on workers, thus failing to address ergonomic hazards. Researchers have proposed combining metal with polymers to create flexible composites. Polymers are lightweight, flexible, cost-effective, and non-toxic, and they can form durable composites with metals that provide excellent mechanical strength and radiation attenuation. Although lighter, these composites can effectively absorb or scatter radiation due to the metal embedded within the polymer matrix.[1,10,11]

While past research has explored materials like tungsten, iron, and bismuth, limited studies have investigated the combination of tin (Sn) with silicone polymers like polydimethylsiloxane (PDMS). Tin, with a high atomic number (Z = 50) and density, has promising shielding properties. Silicones, including PDMS, are widely used in medical applications because of their heat resistance, chemical stability, biocompatibility, and versatility[12–15]. This research aims to examine how varying the composition ratios of pure tin and/or tin alloy and PDMS affects the structural integrity of the composites. The resulting composite with compact structures could enhance radiation shielding, potentially reducing the reliance on lead-based PPE in radiology and other photon-ray applications, thus improving safety for patients and healthcare workers.

This manuscript discusses the comprehensive study of the creation of innovative shielding composite materials formed by combining pure tin and tin alloy with PDMS. This novel approach improves radiation shielding capabilities by leveraging the unique qualities of both PDMS and tin. Field Emission Scanning Electron Microscopy (FESEM) was used to carefully analyze the composite's cross-sectional surface structure, providing valuable insights into the material's morphology. The porosity within the composite, which affects its structural integrity, was observed. We also gained a deeper understanding of the composite's chemical interactions by analyzing its chemical bonds using Fourier Transform Infrared Spectroscopy (FTIR). A thorough radiation characterization was carried out to confirm the shielding capability, proving the composite's effectiveness in reducing photon rays. Tin-PDMS composites demonstrate potential as innovative materials for radiation shielding applications.

Porosity and radiation shielding abilities

The wavelength and energy of the radiation, as well as the thickness, atomic number, and density of the shielding material, all affect how effective a composite is. High-density, high-atomic-number materials are widely used because they provide excellent photon radiation attenuation, including lead and tungsten. By combining absorption and scattering, these materials successfully lower the intensity of radiation and prevent it from penetrating.[16–18]

Radiation shielding performance can be measured in the form of Radiation Protection Efficiency (RPE) as shown in Eq. (1).[4,17,19,20] Meanwhile, the radiation attenuation performance can generally be measured from the value of the linear attenuation coefficient (LAC) and mass attenuation coefficient (MAC), as shown in Eqs. (2) and (3).[4,7]

The RPE, LAC, and MAC mathematically are

$$RPE = \left(1 - \frac{I}{I_O}\right) \times 100 \quad (1)$$

$$I = I_O\, e^{-\mu x} \quad (2)$$

$$\mu_m = \frac{\mu}{\rho} \quad (3)$$

Where:

- I = Intensity of transmitted ray
- I_o = Intensity of incident ray
- μ = LAC of the composite at a specific gamma -ray
- x = Thickness of the composite
- μ_m = MAC
- ρ = Density of materials

A path for the radiation beam to travel through is created by pores and gaps in the composite, which also lessens internal composite interaction with the radiation beam and increases the amount of radiation that can pass through the material. Additionally, this causes the composite's overall density to drop. As attenuation efficacy is directly proportional to the material's atomic number and density, radiation intensity reduction will be less effective in a less dense composite with more pores. Furthermore, weak patches where radiation can enter can be created by non-uniform attenuation brought on by the uneven structure with many pores.[21–23] Generally, the porosity of the pores can be calculated from Eq. (3).[24–27]

$$Degree\ of\ porosity = \frac{V_S - V_{ma}}{V_S} \quad (4)$$

Where:

V_S = volume of composite
V_{ma} = volume of materials

Metal and polymer composites against radiation

Finding the best material for polymers and metals is essential to obtain compact composites with excellent characteristics for radiation shielding. Inorganic polymer-based metal is stated to be the best combination and alternative composite for radiation shielding. Adding metal particles into the polymer matrix can enhance the composites' mechanical, electrical, thermal, and optical properties. The literature highlights the usage of polymers such as epoxy resin, polydimethylsiloxane (PDMS), polypropylene (PP), polyvinyl alcohol (PVA), silicone rubber, and polyvinyl chloride (PVC) combined with metals such as lead (II) oxide (PbO), lead (IV) oxide, cadmium oxide (CdO), bismuth (Bi), tungsten (W), and lead (Pb).[28–31]

The reported study stated that the composites of lead mixed with epoxy resin showed enhanced properties in shielding materials at low-energy gamma rays (60 keV). The study also stated that a polymer with high density and a metal with high density produced an improved composite for radiation shielding.[19] Besides, another study also mentioned that as the energy of gamma rays increases, LAC decreases due to the changes in photon interaction and energy behavior. The study also includes the findings describing the increase in LAC as the concentration of metal filler increased (lead oxide).[6] From the studies, the hypothesis that could be generated is that the highest concentration of metal filler can provide enhanced shielding properties. However, this also depends on the radiation energies used and the density of the materials used.

Another study observed the radiation characteristics of a combination of polyester resin with barium pyrophosphate and barium zirconate, respectively.[2] The highest density (1.3766 g cm^{-3}) mixture, which is 20% barium zirconate, revealed the best LAC (0.0575 cm^{-1}) compared to 20% barium pyrophosphate, with a density of 1.3285 g cm^{-3} recorded the LAC value of 0.0531 cm^{-1} at 1408 keV. There is a slight difference between both composites, which confirms the higher density will provide better attenuation capabilities. However, at low energy of 81 keV, 5% barium pyrophosphate observed LAC is 0.2762 cm^{-1} compared to 5% barium zirconate which is 0.2644 cm^{-1}.[2]

The dominant photon interaction mechanisms at different energy levels cause LAC for low-density materials to behave differently with photon energy. The LAC of low-density materials is generally higher at low photon energy. The photoelectric effect, which relies heavily on photon energy and atomic number (Z), is mostly responsible for this. The percentage of interacting photons per unit thickness can still be substantial in low-density materials, which increases the attenuation even though they typically have lower atomic numbers. Furthermore, low-density materials like composites may include a matrix that permits secondary interactions, increasing attenuation even more. Because low-energy photons have longer wavelengths, these materials are more likely to scatter and absorb them.[16,32,33]

The LAC of low-density materials decreases with increasing photon energy. This is because Compton scattering, which is more dependent on the material's electron density (number of electrons per unit mass) than on the atomic number, becomes the predominant interaction activity in this energy range.[34] Reduced attenuation results from low-density materials' intrinsic lack of electrons available for photon interaction. Pair generation (over 1.02 MeV) becomes important for very high photon energy and is more effective in materials with greater atomic numbers and densities. Consequently, at these higher energy levels, the LAC for low-density materials is relatively smaller.[19,35,36] This energy-dependent behavior emphasizes how crucial it is to fully understand photon interaction mechanisms when selecting materials for radiation shielding or detection applications.

Materials and methods

Composite preparations

A 5.0 mm thick composite was prepared by adding tin powder as filler at ratios of 10%, 20%, 30%, 40%,

Table 1. Material properties of tin-PDMS-based composites.

Properties	Pure Tin	Copper-tin alloy	PDMS polymer
Symbol	Sn	$Cu_{84}Sn_5$	C_2H_6OSi
Form	Powder	Powder	Liquid
Particle size (APS)	8 μm	74 μm	-
Manufacturer/Supplier	Progressive Scientific Sdn. Bhd.	Sigma Aldrich	HardwareMISE Sdn. Bhd.
Density (g cm^{-3})	7.31	8.8	1.103
Liquid viscosity	-	-	3500 cP
Purity (%)	99.8	-	-
Melting point	231.9 °C	-	-

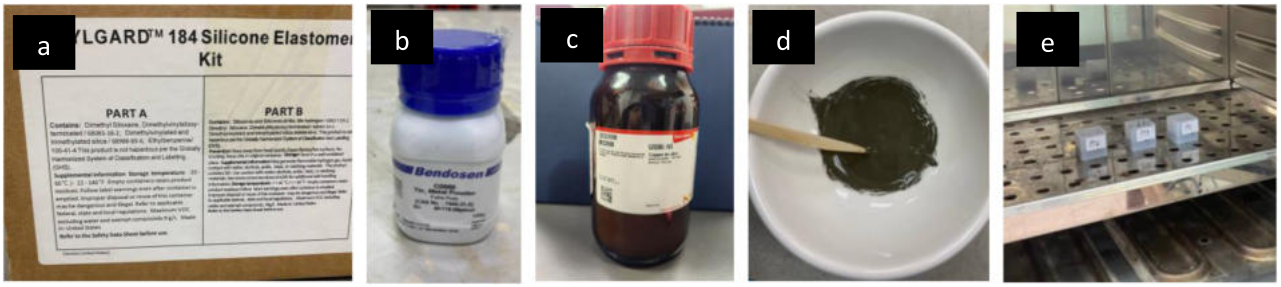

Fig. 1. Polydimethylsiloxane kit (a), pure tin powder (b), copper-tin alloy (c), mixture of metal and polymer (d), and (e) heating process in oven at 100 °C.

50% and 60% metal into the polymer matrix. This study used microparticle-sized pure tin and tin alloys with copper compositions, besides PDMS. The PDMS polymer functions as a binder to the tin powder. The PDMS elastomer liquid contains dimethyl siloxane; dimethylvinylsiloxy-terminated, dimethylvinylated, and trimethylated silica; ethylbenzene with a curing agent containing siloxanes and silicones di-Me, Me hydrogen, dimethylsiloxane, dimethylvinylsioxy-terminated, dimethylvinylated, and trimethylated silica.

Table 1 shows the details of the raw material used. The pure tin powder and the copper-tin alloy are purchased from Progressive Scientific Sdn. Bhd and Sigma Aldrich, respectively. For the PDMS polymer liquid, the Sylgard 184 Kit Set is purchased from HardwareMISE Sdn. Bhd., which consists of PDMS elastomer and PDMS curing agent.

Table 2 shows the tin's composition ratio in the composite and its label. In the composite preparation, the tin powder is added using the weight composition ratio according to the calculation, with various compositions performed Table 2. The PDMS liquid and curing agent were mixed into the ceramic bowl containing pure tin and tin alloy powder. Both ingredients were stirred at the optimum speed to ensure the powder could be dispersed evenly throughout the polymer matrix. The mixture was poured into the mold with the dimensions of 2.0 cm x 2.0 cm x 0.5 cm. The preparation process occurred at room temperature. The initial curing process was done in a glass-vacuum desiccator to degas the air before being cured in a dry oven at 100 °C for 35 minutes Fig. 1. Thereafter, the composite mixture was left at room temperature for 30 minutes to cool down before being taken out from the mold Table 3 and put into the closed container.

Table 2. The details of the composites and tin compositions.

Metal	Composition (%)	Label
Pure tin	10	PT1
	20	PT2
	30	PT3
	40	PT4
	50	PT5
	60	PT6
Copper-tin alloy	10	TA1
	20	TA2
	30	TA3
	40	TA4
	50	TA5
	60	TA6
Copper-tin alloy and pure tin	10 (8 and 2)	PA1
	20 (16 and 4)	PA2
	30 (24 and 6)	PA3
	40 (32 and 8)	PA4
	50 (40 and 10)	PA5
	60 (48 and 12)	PA6

Composite analysis

The composites fabricated from tin and PDMS were characterized using several techniques. Chemical bonding and molecular interactions were detected

Table 3. The overview of the composites.

Composite group	Control	PT1	PT2	PT3	PT4	PT5	PT6
PT		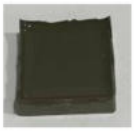			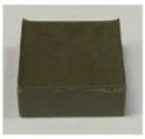		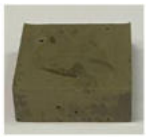
Composite group	**Control**	**TA1**	**TA2**	**TA3**	**TA4**	**TA5**	**TA6**
TA				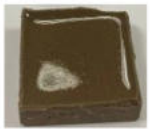		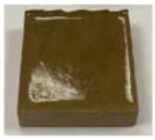	
Composite group	**Control**	**PA1**	**PA2**	**PA3**	**PA4**	**PA5**	**PA6**
PA				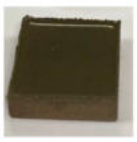	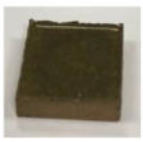		

using Universiti Putra Malaysia's (UPM) Fourier Transform Infrared Spectroscopy (FTIR) facilities. High-resolution imaging was obtained using Field Emission Scanning Electron Microscopy (FESEM) at the Usains Biomics Laboratory, Universiti Sains Malaysia, to examine the surface morphology, pore distribution, and microtin dispersion inside the polymer matrix. ImageJ software was used to quantify porosity. At Universiti Kebangsaan Malaysia (UKM), radiation characterization was carried out using gamma-ray spectroscopy with a Cadmium-109 source. The shielding effectiveness of the composite was assessed by measuring radiation protection efficiency (RPE) and linear attenuation coefficients (LAC). These examinations can determine the composite's potential for successful radiation shielding applications.

Results and discussion

FTIR analysis of the tin-PDMS composite

The graph in Fig. 2 displays the FTIR spectral data for four (4) distinct composites, designated as control, PT6, TA6, and PA6. The y-axis scales from 0 to 1.2, indicating transmittance intensity, and the x-axis ranges from 0 to 4500, representing wavenumbers (cm^{-1}). The materials' infrared absorption spectra show distinct peaks correlating to chemical motions, like bond stretching and bending. These peaks reveal important information about the materials' general composition, molecular structures, and chemical bonding.[1,2,5,37]

When selecting materials for various applications where certain physical and chemical properties are crucial, these FTIR data are crucial. Different absorption peaks can be seen in the FTIR spectra of different composite materials, especially in the 500 to 1500 cm^{-1} range. Usually, the vibrational modes of the polymer backbone and associated metal compounds are linked to these peaks. The Si-O and Si-CH_3 regions of the control spectrum exhibit characteristic peaks, indicating a slight absorption by the pure polymer matrix. But because pure tin is embedded in PDMS, the orange line, which stands for PT6, has the lowest absorbance throughout the spectrum, particularly in the 1000 to 2000 cm^{-1} region, and it exhibits changes in the spectra due to the presence of pure tin embedded in PDMS compared to PDMS spectra.

The reduced transmittance of the metal-containing composites (PT6, TA6, and PA6), especially in the 500 to 2000 cm^{-1} range, indicates that the metals' presence and interactions with PDMS have increased absorption.[1,37,38] The PA6 composite exhibits the most complicated spectrum, as it contains pure tin in PDMS as well as copper-tin alloy. This suggests that the transmittance characteristics are altered by the synergistic effects of the two metals cooperating in the PDMS matrix. The FTIR spectra show that the addition of pure tin and copper-tin alloy significantly alters the transmittance characteristics of the PDMS matrix.

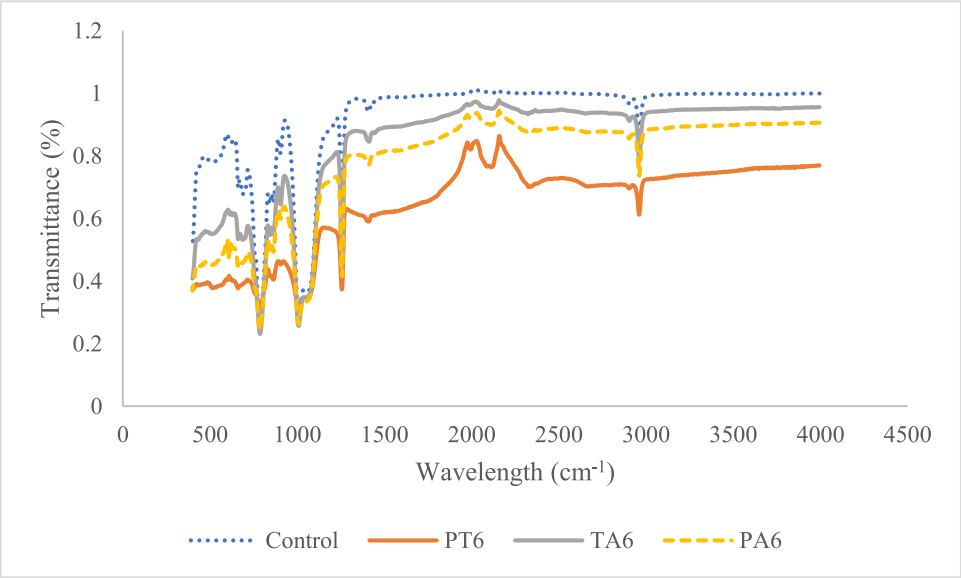

Fig. 2. FTIR spectra for 60% metal filler composites representative of each set and control.

PT6 has the lowest absorbance across the spectrum, indicating a simpler molecular structure, possibly due to weaker C–H or Si–O bonds typical of PDMS-based materials. The grey line, representing TA6, displays the highest absorption. The more prominent peaks observed in 1000 to 1500 and 2000 to 2500 cm^{-1} reflect stronger molecular vibrations and more complex interactions between the copper-tin alloy and the PDMS matrix. Combining the characteristics of pure tin and the copper-tin alloy, PA6's absorption spectrum falls between those of PT6 and TA6. Because of the alloy component, its absorbance is higher than that of PT6, indicating the presence of more or stronger bonds.

These FTIR data are important for choosing materials for various applications where certain physical and chemical characteristics are essential. For example, TA6 may be a favorable choice for coatings or composite materials that require outstanding mechanical strength, thermal stability, or chemical resistance due to its stronger absorbance and more complicated molecular structure. However, PT6 might be more suited for uses that need a less complex, less reactive substance, possibly in settings where low chemical reactivity is preferred. Because of its hybrid approach, PA6 may exhibit moderate strength and reactivity, which makes it perfect for applications requiring a balance of qualities, including intermediate coatings or flexible electronics.

To sum up, the FTIR spectra of PT6, TA6, and PA6 show notable variations in their bonding and molecular structures. TA6 is notable for having a greater absorbance, indicating a more complex composition, whereas PT6 shows weaker interactions. With components of both pure tin and copper-tin alloy, PA6 provides a compromise. It is essential to comprehend these distinctions when choosing materials for different industries based on desired qualities like mechanical strength, flexibility, or chemical resistance.

Morphological study of the tin-PDMS composite

Fig. 3 illustrates the FESEM image for the control PDMS composite with 0% tin enrichment. Figs. 4 to 6 illustrate the cross-sectional FESEM image of homogenously distributed tin filler within the PDMS matrixes. The FESEM morphology revealed the distribution homogeneity of pure tin and tin alloy microparticles across the PDMS matrixes. From the image, the pore inside the composites can be seen produced adjacent to the large particle, which may reduce the effectiveness of the composite in shielding against radiation rays.[39] The distribution of pores was not uniform and was observed at high composition of tin powders.

The structural integrity of the microparticles within the polymer matrix shows higher integrity in the mixture of PA than in the PT and TA composite. This might be due to the high concentration of high-density powders in the tin alloy. As the composition increased, the density increased Table 4. The PA was recorded as having the highest density compared to the tin alloy-PDMS and pure tin-PDMS. The high density significantly affects the radiation shielding properties of the composites. According to the FESEM

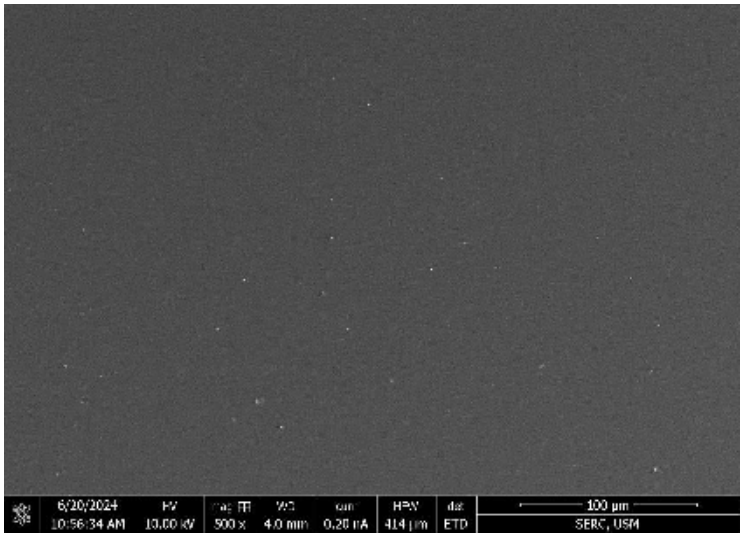

Fig. 3. FESEM images PDMS control image at 500x magnification.

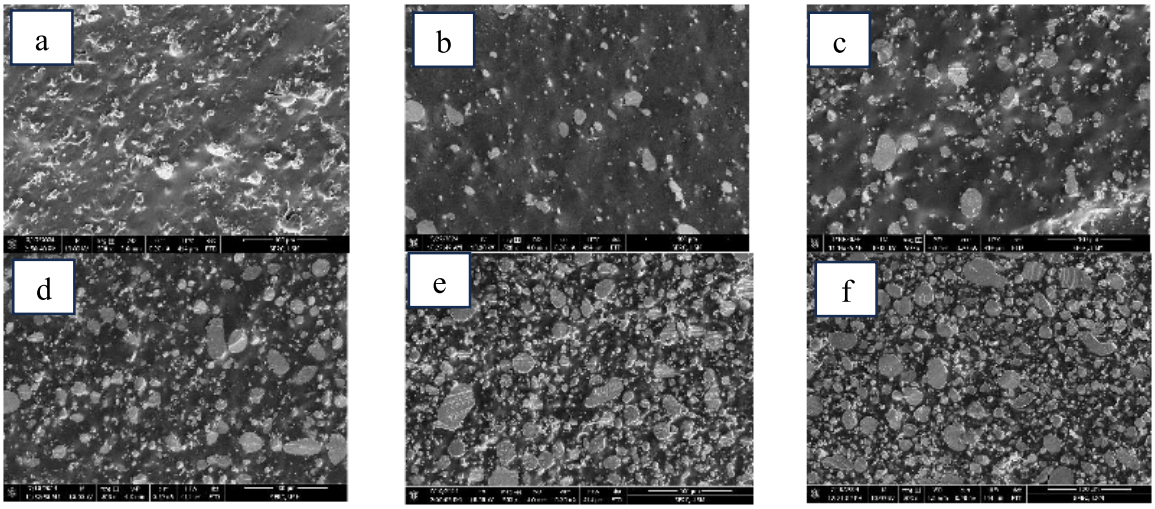

Fig. 4. FESEM images at 500x magnification of the tin-PDMS composite enriched with pure tin: a) PT1, b) PT2, c) PT3, d) PT4, e) PT5, and f) PT6.

images shown in Figs. 4 to 6, an increase in metal compositions resulted in a higher number of homogenously distributed metal particles within the polymer matrix.

Porosity of the tin-PDMS composite

ImageJ was used to analyze the FESEM images to obtain the percentage of porosity. Fig. 7 shows an example of the ImageJ analysis on the FESEM image of the TA6 composite. Table 4 demonstrates the percentage of porosity, and Fig. 8 illustrates the percentage of porosity in the line graph.

The composite's ability to reduce radiation intensity decreases when the composites are porous and not compact. Radiation can travel through the composite's pores and gaps with minimal interaction within it. It lessens the interaction between the radiation beams passing through these pores, minimizing scattering and absorption. As a result, the material can absorb more radiation beams without attenuating them, which lowers the shielding's overall efficiency.[40–43] Therefore, the existence of the pores was thoroughly examined by analyzing FESEM images using ImageJ software. Measurement of the pore diameters in the composites and calculation of the porosity % can be obtained using ImageJ.[39,44]

More atoms are present to absorb, scatter, or attenuate the radiation when there is a higher density. Fewer atoms per unit volume attenuate radiation

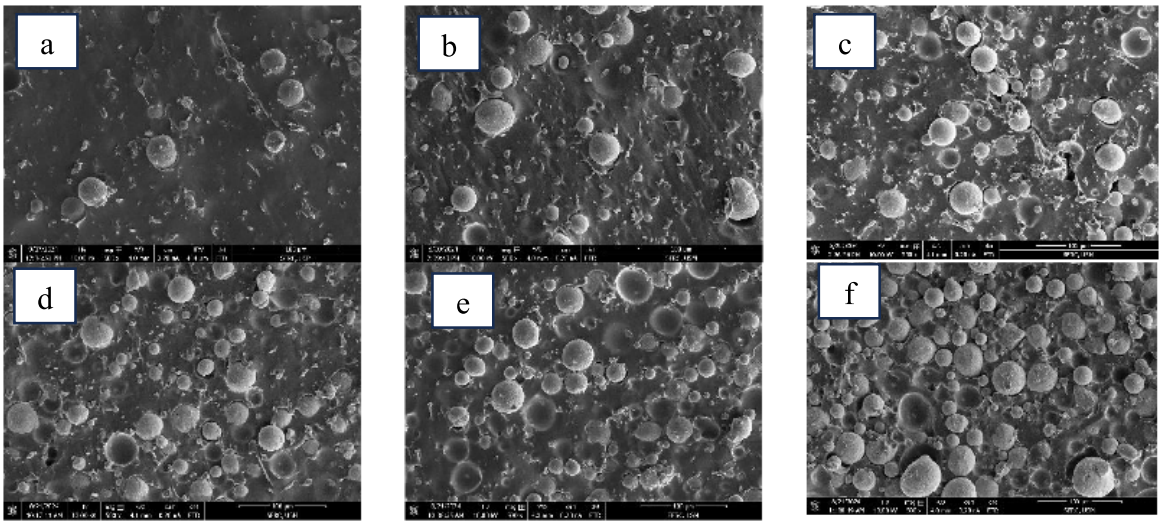

Fig. 5. FESEM images at 500x magnification of the tin-PDMS composite enriched with tin alloy a) TA1, b) TA2, c) TA3, d) TA4, e) TA5, and f) TA6.

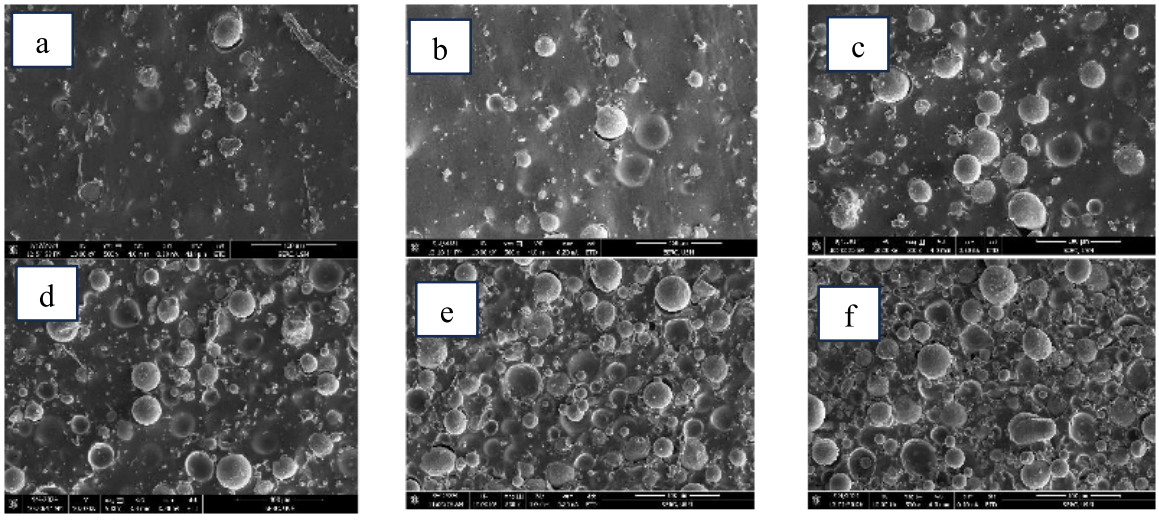

Fig. 6. FESEM images at 500x magnification of the tin-PDMS composite enriched with a mixture of pure tin and tin alloy: a) PA1, b) PA2, c) PA3, d) PA4, e) PA5, and f) PA6.

when density is decreased because of porosity, which reduces the material's ability to function as a shield. Furthermore, attenuation efficiency and the material's density and atomic number are tightly linked. Radiation intensity reduction will be less effective with a less dense composite that has many pores. The atomic number of each atom in a composite interaction determines the radiation and atoms involved. Lead and other high-atomic-number metals work well because they offer a higher chance of interactions per unit volume.[45] When the composite is porous, its capacity to shield against radiation is compromised due to an effective drop in the atomic number and effective density.[40,41,43]

In addition, radiation may be able to pass through more easily due to non-uniform attenuation brought on by the uneven structure with many pores. The areas of reduced attenuation efficiency caused by these weak spots reduce the overall effectiveness of the shield. The material structure's diversity can result in unpredictable performance, which reduces the composite's dependability as a radiation shield.[40] This analysis indicates that the maximum porosity percentage is 2.16% Table 4. The overall porosity, the density of the material, and the kind of radiation to be attenuated are some of the parameters that will affect how efficient the material is at attenuating radiation. Even tiny cracks can significantly affect attenuation

Table 4. The density and percentage of porosity recorded for each sample.

Composites	Ratio (Polymer: Metal)	Density (g cm^{-3})	Percent of the porosity (%)
PT1	9:1	1.607	0.26
PT2	8:2	2.066	0.08
PT3	7:3	2.915	0.05
PT4	6:4	3.395	0.47
PT5	5:5	4.000	0.09
PT6	4:6	4.500	0.69
TA1	9:1	1.786	0.41
TA2	8:2	2.455	1.35
TA3	7:3	3.235	1.56
TA4	6:4	3.941	2.16
TA5	5:5	4.770	0.70
TA6	4:6	5.505	1.67
PA1	9:1	1.827	0.13
PA2	8:2	2.520	0.33
PA3	7:3	3.578	0.24
PA4	6:4	3.800	0.32
PA5	5:5	4.595	1.09
PA6	4:6	5.553	1.38

if the composites have numerous pores to provide a high overall porosity. [34,40,44]

Small pores can have different effects according to the kind of radiation. For example, small porosity may affect gamma rays and other high-energy photons less than low-energy photons or particles. Materials are more prone to absorb high-energy radiation, and tiny pores may not have a major impact on this interaction. However, since there is a greater interaction between low-energy photons and the material in the case of low-energy radiation, even tiny gaps can result in weak patches that lower the overall efficiency of attenuation. [40–43]

Fig. 8 illustrates intriguing patterns in the structural behavior of three materials (PT, TA, and PA) based on their porosity data at different metal concentrations, as observed in 500x magnification images from FE-SEM. The porosity of TA showed the most significant variations, rising gradually to a peak at 40% metal concentration, then sharply declining at 50%, and then increasing again at 60%. This non-linear pattern implies that other factors, including material interactions or manufacturing processes, are influencing the porosity in addition to the mere metal content. From 10% to 30%, PA's porosity levels were fairly constant, but, similar to TA, they then sharply increased at 40%, decreased slightly at 50%, and then increased again at 60%. This pattern would suggest that it is difficult to distribute the metal uniformly throughout the polymer, which would result in increased porosity at elevated metal concentrations.

As a result of its superior resistance to metal addition and possibly more stable interaction between the metal and polymer matrix, PT, on the other hand, maintained the lowest and most constant porosity levels across all metal concentrations. Even with its minor increase to 60%, the porosity in PT was still far lower than the peaks seen in TA and PA. This implies that, in comparison to the other two materials, PT may have superior structural stability when mixed with metal content.

Copper-tin alloy particles were observed under FE-SEM Fig. 5 and revealed the spherical structures with an average size of 74 μm compared to the pure tin particle size of 8 μm. The composites using copper-tin alloy as the metal filler revealed peel-off structures and increased pores within the polymer matrixes. The particles' spherical shape may have allowed them to slide out of the polymer matrices. In addition, the peeling off of the copper particles leads to increased pores and a weak structure of the composites for radiation shielding purposes.

Overall, the porosity did not rise linearly with the amount of metal, suggesting that natural porosity formation, particularly in TA and PA composites, may occur during the composite's fabrication process. Uneven metal particle distribution, insufficient mixing, and air bubble entrapment inside the PDMS matrix during the curing process are some of the likely causes of this natural occurrence of porosity. Higher metal filler causes the composite mixture's viscosity to rise, making it harder for trapped air to escape and leading to the creation of pores and voids. Furthermore, the existence of metal agglomerates or clusters may result in micro gaps that enhance porosity.

Porosity control may also be enhanced by more research into alternative fabrication techniques, including hot pressing, extrusion, or the use of additives. Additionally, investigating the molecular interactions between the polymer and metal at different resolutions may provide information on how to best optimize composite integrity and metal dispersion.

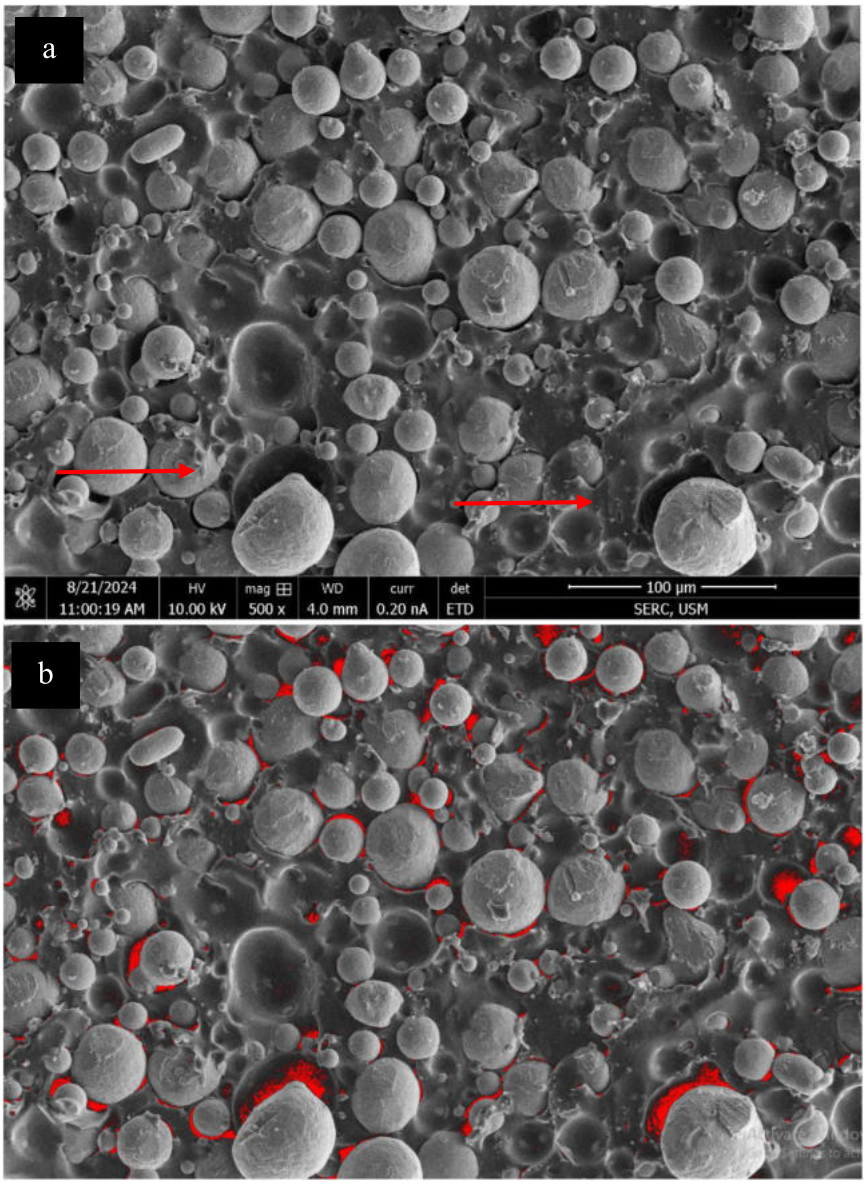

Fig. 7. TA6 (a) at 500x magnification with the red arrow (the formation of pores due to peeling off of the particles) and after analysis for percentage of porosity using ImageJ.

In summary, porosity appears to result more naturally from the manufacturing process than from the amount of metal used; however, specific modifications to fabrication methods may enhance the results and structural stability of porosity. [46–49]

Additionally, examining whether the distribution of particle sizes affects porosity could provide beneficial data. There can be fewer gaps if the particles are smaller or more evenly distributed. Another option is to investigate the use of nanoparticles, which may combine more easily with the polymer and reduce porosity while simultaneously enhancing the mechanical characteristics of the composite. Altering the metal particles' surface is an additional choice. The adhesion between metal and polymer can be improved by coating the particles with a coupling agent, such as silane, or by applying chemical treatments, like oxidation, which will result in a denser and more uniform structure.

Radiation attenuation parameters for the tin-PDMS composite

To determine effective composite materials that shield against ionizing radiation, two crucial metrics are the LAC and radiation protection efficiency (RPE).

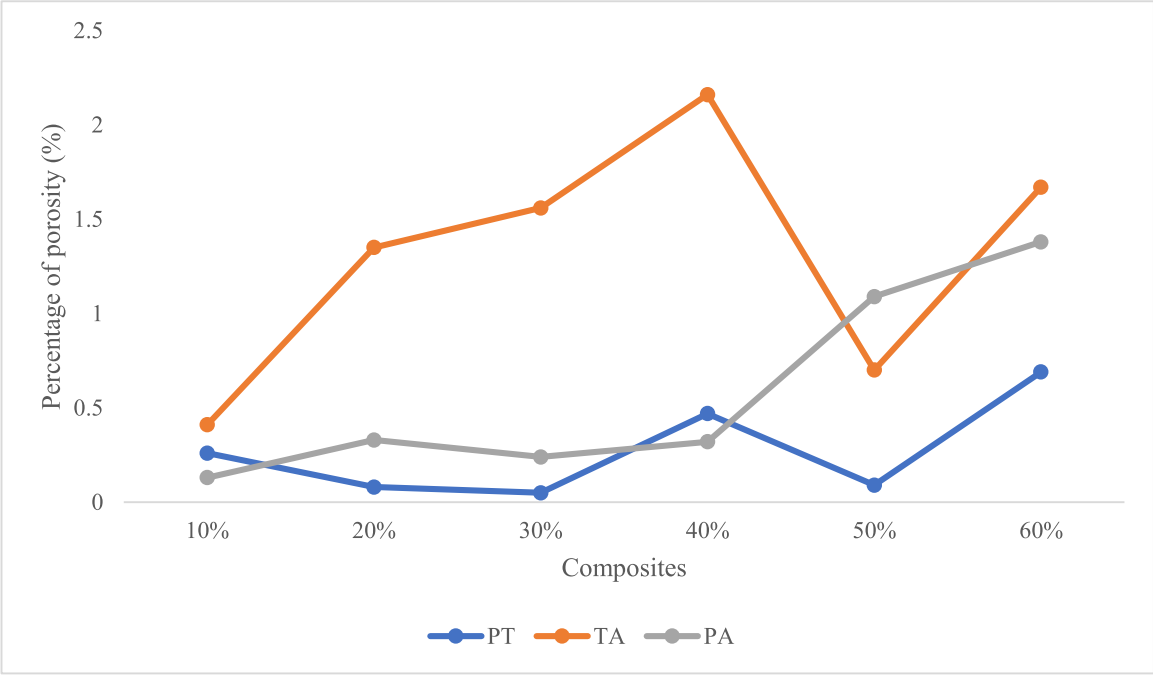

Fig. 8. Percentage of porosity for each composite.

Whereas the RPE shows the proportion of radiation that the material can absorb or scatter, the LAC measures the material's capacity to attenuate radiation per unit thickness. The concentration of tin and tin alloy in the PDMS matrix was found to increase both LAC and RPE in this investigation. This pattern is explained by tin's larger atomic number and density, which increases the likelihood of photon interaction processes, including Compton scattering and photoelectric absorption. On the other hand, lower LAC and RPE indicate a weaker radiation attenuation capacity when shielding material concentration is lower.[19,50,51]

The graph in Fig. 9 demonstrates the control lead (CL) and how the concentration of metal in three (3) different mixtures of metal-polymer composites, which are PT, TA, and PA, relates to RPE. In all three composites, the RPE generally rises with metal concentration, demonstrating the improved shielding ability offered by a larger metal content. This pattern is explained by the fact that larger metal concentrations result in denser materials, which enhance radiation attenuation via processes like photoelectric absorption and scattering.[17,19,52]

PT continuously exhibits the greatest RPE among the composites at all concentrations, comparable to CL. Tin's high atomic number and density, which enable it to interact with and attenuate photon radiation very effectively, serve as the reason for this. Although it performs slightly less effectively than PT, the PA composite outperforms TA. Compared to the alloy alone, the synergistic effect of pure tin and copper-tin alloy enhances attenuation qualities. Because copper has a lower atomic number than tin, it is less effective at photon interaction, which is why the TA composite shows the lowest RPE at all concentrations.[52,53]

At lower concentrations, such as 10%, there is less metal available for attenuation, resulting in comparatively low RPE for all composites. The performance of the TA composite is greatly enhanced with the addition of pure tin, and the variations between the composites become more noticeable as the concentration rises to 20 to 30%. The RPE peaks for all composites are at greater concentrations of 40 to 60%, with PT continuing to perform better. With PT being the most effective and the PA composite coming in second, these results emphasize the significance of both metal type and concentration in affecting the shielding performance of metal-polymer composites.[28,52]

In metal-polymer composites, the relationship between porosity and RPE is complex and can change based on several variables. Although porosity can affect the density and structure of a material, other important factors like the material's composition, how metal particles interact with the polymer matrix, and the radiation source's energy frequently have a greater effect on RPE. Because of this, it is crucial to thoroughly examine the data without presuming that porosity and RPE are directly correlated.[16,23,25,33]

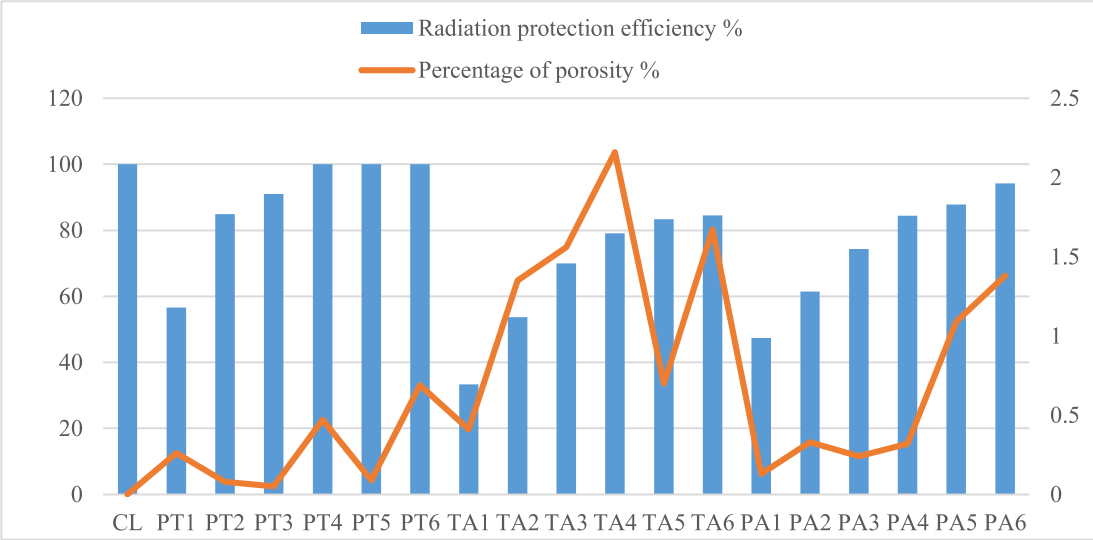

Fig. 9. Radiation protection efficiency (RPE) at 88 keV and percentage of porosity against the different metal concentrations of the composites.

Porosity does not directly affect RPE, but it can lower material density and disrupt structural integrity. The RPE of composites TA4 and PA6, for instance, differs greatly while having larger porosity values (up to 2%), indicating that material composition is more important than porosity alone.

This association is further highlighted by the dual-axis graph Fig. 9, which compares porosity (%) and RPE (%) across composites. For PT4, PT5, PT6, and PA6, high RPE values are noted, signifying superior shielding performance. Conversely, composites like PT1 and TA1 with lower RPE typically have lower shielding efficiency. PA6 can retain high RPE despite increasing porosity, proving the significance of elements like atomic structure and material composition.

Although TA and PA have higher densities, their RPE is lower than PT's. This is primarily attributable to the materials' composition. Tin, which has a larger atomic number, interacts more effectively with photon radiation through methods such as photoelectric absorption. Despite its low density, the prevalence of tin in PT's composition improves its shielding efficiency. In contrast, TA, which contains a significant amount of copper, a lower-Z material, is less effective at photon attenuation even at higher densities. PA outperforms TA because of the presence of pure tin, although it still falls short of PT in terms of RPE.[11,19,51,54]

While density is an important factor in radiation shielding, it alone is not sufficient to guarantee high RPE. Material composition, particularly the inclusion of high-Z elements like tin, plays a more critical role. Porosity further complicates the relationship, as even high-density materials with significant porosity may underperform compared to low-density materials with minimal porosity. This illustrates the value of considering both structural and compositional factors when designing effective radiation shielding composites.

Table 5. The linear attenuation coefficients (LAC) of the composites.

Composites	LAC (cm^{-1})
CL	∞
PT1	1.8154
PT2	3.6402
PT3	4.6271
PT4	∞
PT5	∞
PT6	∞
TA1	0.8256
TA2	1.5709
TA3	2.3585
TA4	3.0058
TA5	3.4454
TA6	3.5186
PA1	1.3111
PA2	2.0300
PA3	2.5152
PA4	3.6482
PA5	4.0413
PA6	1.3111

The TA composite shows lower RPE and LAC values than PT. The LAC values Table 5 are between 0.8256 cm^{-1} (TA1) and 3.5186 cm^{-1} (TA6), and RPE is gradually getting better but still not attenuating completely. The decreased atomic number and density of the TA in comparison to PT are the reasons for the decrease in radiation shielding

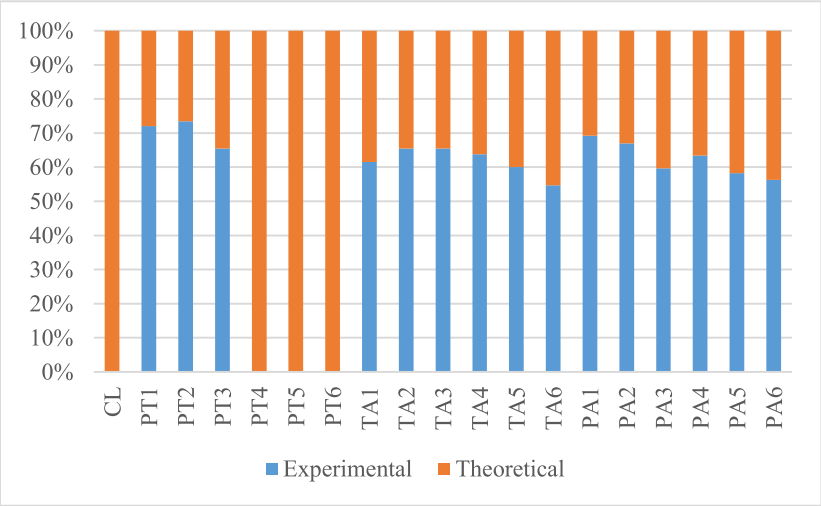

Fig. 10. Experimental and theoretical (XCOM) values of mass attenuation coefficients at 88 keV.

performance. Nonetheless, the steady rise in LAC and RPE of TA with increasing metal concentrations indicates the alloy's potential for moderate shielding applications.

In both LAC and RPE, the PA composite performs better than the TA, reaching values that are more in line with the TA. With high RPE percentages and LAC values peaking at 5.074 cm^{-1} (PA6), this composite gains from the alloy's and tin's combined contributions. The hybrid composite preserves better mechanical and processing properties while improving shielding performance. Since less porosity reduces photon leakage and scattering, the PA composites' lower porosity is probably a factor in their better performance. [23,55]

The CL sample's occurrence of an infinite (∞) LAC value further confirms the precision of the utilized technique and the sensitivity of the experimental setup. Lead's high density and atomic number allow it to effectively attenuate gamma radiation, making it a well-known and frequently used radiation shielding material. When CL displays an infinite LAC value, the radiation intensity was either zero or below the equipment's detection threshold after it had passed through the lead sample.

Since lead may absorb almost all incident photons, this result is expected under specific circumstances, particularly at lower gamma-ray energy and a sufficiently thick sample. When inserted into the LAC formula, any instance where the transmitted intensity approaches zero causes the logarithmic term to approach infinity. CL, PT4, PT5, and PT6 all displayed infinite LAC values during the experiment, indicating that these materials were very successful at attenuating radiation. The similar performance of PT4 to PT6 shows the outstanding potential of tin-based PDMS composites as lead-free substitutes, even if CL is the standard for optimum shielding efficiency. This is especially important for applications that need radiation shielding materials that are flexible, non-toxic, and eco-friendly.

There is a clear association between LAC and RPE for all materials. Higher RPE is consistently correlated with higher LAC values, suggesting that both measures accurately capture the shielding effectiveness of the composite. [1,28,33] The absolute values are influenced by variations in porosity, density, and material composition, denser and less porous materials. While the balanced performance of PA indicates it may be more adaptable for wider use cases, the total attenuation seen in PT4 to PT6 emphasizes the better potential of pure tin composites for applications demanding maximal shielding effectiveness.

The mass attenuation coefficient (MAC) values in Fig. 10 for the samples are displayed in the bar chart according to theoretical calculation and experimental measurements (by gamma-ray spectroscopy and the XCOM database, respectively). The experimental measurement showed a 0% MAC, specifically for CL PT4, PT5, and PT6. Gamma-ray spectroscopy revealed no photon transmission and 100% shielding efficacy.

In comparison to the theoretical calculations, the experimental MAC values (XCOM data) for the other samples, such as the PT, TA, and PA groups, consistently showed larger percentages. This implies that the composites' real shielding performance exceeded theoretical expectations. Several variables that were not fully taken into consideration in theoretical models, including density variations in the composites, the thicknesses, microstructural flaws, filler distribution uniformity, and the existence of

interfacial gaps within the polymer matrix, may have an impact on the discrepancies between theoretical and experimental results.[17,33,56]

Furthermore, it is found that the PT group consistently maintains higher MAC values than the TA and PA groups among the various sample groups. This is to be expected given that pure tin has a higher atomic number and a greater photon interaction probability than alloys.[17,33,56] The experimental findings support the effective creation of the composites for improved radiation shielding, which is in good agreement with theory but shows marginally better performance in practice.

This approach generally illustrates the importance of confirming theoretical calculations with experimental data while creating new radiation shielding materials. To sum up, the correlation between LAC, MAC, and RPE emphasizes how crucial material density, composition, and porosity are in determining shielding effectiveness. The PA composite provides a competitive alternative with improved material properties, making it a promising material for practical applications and radiation shielding applications, even if PT achieves the best effectiveness.

Conclusion

This study emphasizes the theoretical benefits of tin-based composites in radiation shielding applications. The study of the relationship between metal content and porosity in metal-polymer composites revealed that increasing metal concentration affects porosity. The higher metal concentration significantly improves the composite's capacity to attenuate radiation, despite its large porosity. This suggests that metal content, rather than porosity, is more important for shielding efficacy. Nonetheless, by eliminating voids, external pressure throughout the fabrication process may be beneficial in lowering porosity. To improve the overall structural integrity of composites, further research should be conducted using approaches such as surface-modified metal particles, hybrid filler combinations, and polymers. PT had the highest radiation shielding efficiency because of its high atomic number, low porosity, and excellent photon interaction characteristics. Increased porosity and copper's reduced attenuation capabilities restricted the performance of TA and PA composites, despite their higher densities. The addition of tin to PA enhanced its performance relative to TA, but it did not outperform PT. A structural study indicated that porosity is crucial in determining composite efficiency, as larger porosity disrupts photon attenuation pathways, limiting shielding performance. For application, these solutions may provide more efficient methods of lowering porosity and enhancing structural integrity in metal-polymer composites. This work provides the basis for future research to improve the efficiency and application of metal-polymer composites in radiation protection.

Acknowledgment

The authors express their gratitude to the Ministry of Higher Education (MOHE) for financial support provided through the Fundamental Research Grant Scheme (FRGS/1/2023/STG05/UITM/03/3). Appreciation is also extended to Universiti Teknologi MARA Cawangan Pulau Pinang for granting access to workstation facilities and for their valuable assistance. The authors acknowledge Usains Biomics Laboratory Testing Services Sdn Bhd, Universiti Sains Malaysia, for providing the facilities for FESEM imaging. Acknowledgment is also extended to Universiti Putra Malaysia (UPM) for Fourier Transform Infrared Spectroscopy (FTIR) analysis services and to Universiti Kebangsaan Malaysia (UKM) for providing facilities for radiation characterization.

Authors' declaration

- Conflicts of Interest: None.
- We hereby confirm that all the figures and tables in the manuscript are ours. Furthermore, any figures and images that are not ours have been included with the necessary permission for republication, which is attached to the manuscript.
- No animal studies are present in the manuscript.
- No human studies are present in the manuscript.
- Ethical Clearance: The project was approved by the local ethical committee at Universiti Teknologi MARA Cawangan Pulau Pinang, 13500 Permatang Pauh, Pulau Pinang, Malaysia.

Authors' contribution statement

H.Z.A. wrote the full manuscript. H.Z.A. and N.M.A.M. wrote the original draft preparation and editing. H.Z.A., N.S.R., N.I.N.I., and A.Z.S. were involved in data contribution. Data analysis was done by H.Z.A., N.M.A.M., and N.A.A.W. Revision and supervision by R.Z., A.M., and N.A.A.W. All authors have read and agreed to the published version of the manuscript.

Funding statements

The authors express their gratitude to the Ministry of Higher Education (MOHE) for financial support

provided through the Fundamental Research Grant Scheme (FRGS/1/2023/STG05/UITM/03/3).

References

1. Mahmoud ME, El-Khatib AM, Badawi MS, Rashad AR, El-Sharkawy RM, Thabet AA. Fabrication, characterization and gamma rays shielding properties of nano and micro lead oxide-dispersed-high density polyethylene composites. Radiat Phys Chem. 2018;145:160–173. https://doi.org/10.1016/j.radphyschem.2017.10.017.
2. Ozel F, Akman F, Kaçal MR, Ozen A, Arslan H, Polat H, *et al.* Production of microstructured BaZrO3 and Ba2P2O7-based polymer shields for protection against ionizing photons. J Phys Chem Solids. 2021;158:110238. https://doi.org/10.1016/j.jpcs.2021.110238.
3. Almuqrin AH, Alasali HJ, Sayyed MI, Mahmoud KG. Preparation and experimental estimation of radiation shielding properties of novel epoxy reinforced with Sb2O3 and PbO. E-Polymers. 2023;23(1). https://doi.org/10.1515/epoly-2023-0019.
4. Gouda MM, Abbas MI, Hammoury SI, Zard K, El-Khatib MA. Nano tin oxide/dimethyl polysiloxane reinforced composite as a flexible radiation protecting material. Sci Rep. 2023;13(1):1–13. https://doi.org/10.1038/s41598-023-27464-z.
5. Aladailah MW, Tashlykov OL, Volozheninov TP, Kaskov DO, Iuzbashieva KS, Al-Abed R, *et al.* Exploration of physical and optical properties of ZnO nanopowders filled with polydimethylsiloxane (PDMS) for radiation shielding applications. Simulation and theoretical study. Opt Mater. 2022;134:113197. https://doi.org/10.1016/j.optmat.2022.113197.
6. Elsafi M, Al-Ghamdi H, Sayyed MI, Antar A, Almuqrin AH, Mahmoud KA, *et al.* Optimizing the gamma-ray shielding behaviors for polypropylene using lead oxide: A detailed examination. J Mater Res Technol. 2022;19:1862–1872. https://doi.org/10.1016/j.jmrt.2022.05.128.
7. El-Khatib AM, Abbas MI, Hammoury SI, Gouda MM, Zard K, Elsafi M. Effect of PbO-nanoparticles on dimethyl polysiloxane for use in radiation shielding applications. Sci Rep. 2022;12(1):1–13. https://doi.org/10.1038/s41598-022-20103-z
8. El-Sharkawy RM, Abdou FS, Gizawy MA, Allam EA, Mahmoud ME. Bismuth oxide nanoparticles (Bi2O3 NPs) embedded into recycled-Poly(vinyl chloride) plastic sheets as a promising shielding material for gamma radiation. Radiat Phys Chem. 2023;208:110838. https://doi.org/10.1016/j.radphyschem.2023.110838
9. El-Khatib AM, Elsafi M, Almutiri MN, Mahmoud RMM, Alzahrani JS, Sayyed MI, *et al.* Enhancement of bentonite materials with cement for gamma-ray shielding capability. Materials. 2021;14(16). https://doi.org/10.3390/ma14164697.
10. Husain HS, Rasheed Naji NA, Mahmood BM. Investigation of gamma ray shielding by polymer composites. IOP Conf Ser Mater Sci Eng. 2018;454(1):012131. https://doi.org/10.1088/1757-899X/454/1/012131.
11. Ahmed B, Shah GB, Malik AH, Aurangzeb, Rizwan M. Gamma-ray shielding characteristics of flexible silicone tungsten composites. *Appl Radiat Isot.* 2020;155:108901. https://doi.org/10.1016/j.apradiso.2019.108901.
12. Sekiguchi T, Ueno H, Menon VA, Ichige R, Tanaka Y, Toshiyoshi H, *et al.* UV-curable polydimethylsiloxane photolithography and its application to flexible mechanical metamaterials. *Sensors Mater*. 2023;35(2–6):1995–2011. https://doi.org/10.18494/SAM4351
13. Polywka A, Stegers L, Krauledat O, Riedl T, Jakob T, Görrn P. Controlled mechanical cracking of metal films deposited on polydimethylsiloxane (PDMS). *Nanomaterials (Basel)*. 2016;6(9). https://doi.org/10.3390/nano6090168.
14. Ariati R, Sales F, Souza A, Lima RA, Ribeiro J. Polydimethylsiloxane composites characterization and its applications: A review. *J Polym* Res. 2021. https://doi.org/10.3390/polym13234258.
15. Teixeira I, Castro I, Carvalho V, Rodrigues C, Souza A, Lima R, *et al.* Polydimethylsiloxane mechanical properties: A systematic review. *AIMS Mater Sci*. 2021;8(6):952–973. https://doi.org/10.3934/matersci.2021058.
16. Abualroos NJ, Zainon R. Fabrication of new non-hazardous tungsten carbide epoxy resin bricks for low energy gamma shielding in nuclear medicine. *J Phys Commun*. 2021;5(9). https://doi.org/10.1088/2399-6528/ac26de.
17. Abualroos NJ, Yaacob KA, Zainon R. Radiation attenuation effectiveness of polymer-based radiation shielding materials for gamma radiation. *Radiat Phys Chem*. 2023;212:111070. https://doi.org/10.1016/j.radphyschem.2023.111070
18. Alresheedi MT, Elsafi M. Effect of waste iron filings (IF) on radiation shielding feature of polyepoxide composites. *Crystals*. 2023;13(8). https://doi.org/10.3390/cryst13081168.
19. Abualroos NJ, Idris MI, Ibrahim H, Kamaruzaman MI, Zainon R. Physical, mechanical, and microstructural characterisation of tungsten carbide-based polymeric composites for radiation shielding application. *Sci Rep*. 2024;14(1). https://doi.org/10.1038/s41598-023-49842-3.
20. El-Sawy AA, Sarwat E. Comparative study of gamma-ray shielding parameters for different epoxy composites. *Baghdad Sci J*. 2024;21(2):0480–0480. https://doi.org/10.21123/BSJ.2023.7685.
21. Lai F, Li Z, Fu Y, Adenutsi CD. Investigating the effects of pore-structure characteristics on porosity and absolute permeability for unconventional reservoirs. Energy Fuels. 2021;35(1):690–701. https://doi.org/10.1021/acs.energyfuels.0c03152.
22. Zhang Y, Li Z, Wu H. Interactive machine learning for segmenting pores of sandstone in computed tomography images. J Gas Sci Eng. 2024;126:205343. https://doi.org/10.1016/j.jgsce.2024.205343.
23. Anovitz LM, Cole DR. Characterization and analysis of porosity and pore structures. Pore Scale Geochem Process. 2015;61–164. https://doi.org/10.2138/rmg.2015.80.04.
24. Babaei M, Kiarasi F, Asemi K, Hosseini M. Functionally graded saturated porous structures: A review. J Comput Appl Mech. 2022;297–308. https://doi.org/10.22059/JCAMECH.2022.342710.719.
25. Xiao M, Yang F, Im S, Dlamini DS, Jassby D, Mahendra S, *et al.* Characterizing surface porosity of porous membranes via contact angle measurements. J Membr Sci Lett. 2022;2(1). https://doi.org/10.1016/j.memlet.2022.100022.
26. Fauzi NA, Isa IS, Isa SM, Manaf AA, Rahim AFA, Mahmood A, *et al.* Gallium nitride depth porosity using image processing method. IEEE Symp Comput Appl Ind Electron. 2023;198–202. https://doi.org/10.1109/ISCAIE57739.2023.10165126.
27. Isa IS, Isa SM, Abd Manaf A, Abd Rahim AF, Mahmood A, Abdullah MH, *et al.* Morphological and structural characteristics of gallium nitride (GaN) porosity using image processing. Optik. 2022;271:170126. https://doi.org/10.1016/j.ijleo.2022.170126.
28. Kawady NA, Elkattan M, Salah M, Galhoum AA. Fabrication, characterization, and gamma ray shielding properties of PVA-based polymer nanocomposite. J Mater Sci. 2022;57(24):11046–11061. https://doi.org/10.1007/s10853-022-07213-9.

29. Gholamzadeh L, Sharghi H, Aminian MK. Synthesis of barium-doped PVC /Bi_2WO_6 composites for X-ray radiation shielding. Nucl Eng Technol. 2022;54(1). https://doi.org/10.1016/j.net.2021.07.045.
30. Wang J, Zhou H, Gao Y, Xie Y, Zhang J, Hu Y, *et al.* The characterization of silicone-tungsten-based composites as flexible gamma-ray shields. Materials. 2021;14(20). https://doi.org/10.3390/ma14205970
31. El-Khatib AM, Abbas MI, Elzaher MA, Badawi MS, Alabsy MT, Alharshan GA, *et al.* Gamma attenuation coefficients of nano cadmium oxide/high density polyethylene composites. Sci Rep. 2019;9(1):1–11. https://doi.org/10.1038/s41598-019-52220-7
32. Li C, Sun Y, Cheng M, Sun S, Hu S. Fabrication and characterization of a TiO_2/polysiloxane resin composite coating with full-thickness super-hydrophobicity. Chem Eng J. 2018; 333:361–369. https://doi.org/10.1016/j.cej.2017.09.165.
33. Mahmoud ME, El-Sharkawy RM, Allam EA, Elsaman R, El-Taher A. Fabrication and characterization of phosphotungstic acid–Copper oxide nanoparticles–Plastic waste nanocomposites for enhanced radiation-shielding. J Alloys Compd. 2019;803:768–777. https://doi.org/10.1016/j.jallcom.2019.06.290.
34. Mahmoud KA, Lacomme E, Sayyed MI, Özpolat F, Tashlykov OL. Investigation of the gamma ray shielding properties for polyvinyl chloride reinforced with chalcocite and hematite minerals. In Heliyon [Internet]. Elsevier Ltd; 2020 [cited 2025 March 4];6(3). https://doi.org/10.1016/J.HELIYON.2020.E03560.
35. Ambika MR, Nagaiah N, Harish V, Lokanath NK, Sridhar MA, Renukappa NM, *et al.* Preparation and characterisation of Isophthalic-Bi_2O_3 polymer composite gamma radiation shields. Radiat Phys Chem. 2017;130:351–358. https://doi.org/10.1016/j.radphyschem.2016.09.022.
36. Cinan ZM, Erol B, Baskan T, Mutlu S, Yilmaz SS, Yilmaz AH. Gamma irradiation and the radiation shielding characteristics for the lead oxide doped crosslinked polystyrene-b-polyethyleneglycol block copolymers and the polystyrene-b-polyethyleneglycol-boron nitride nanocomposites. J Polym Res. 2021. https://doi.org/10.3390/polym13193246.
37. Yılmaz SN, Güngör A, Özdemir T. The investigations of mechanical, thermal and rheological properties of polydimethylsiloxane/bismuth (III) oxide composite for X/Gamma ray shielding. Radiat Phys Chem. 2020;170:108649. https://doi.org/10.1016/j.radphyschem.2019.108649.
38. Yilmaz M, Pekdemir ME, Özen Öner E. Evaluation of Pb doped Poly(lactic acid) (PLA) /Poly(ethylene glycol) (PEG) blend composites regarding physicochemical and radiation shielding properties. Radiat Phys Chem. 2023;202:110509. https://doi.org/10.1016/j.radphyschem.2022.110509.
39. Zainal Abidin H, Mukhtar NMA, Mahmood A, Abdul Wahab NA, Zainon R, Roslan NS, *et al.* Effect of tin filler composition on porosity in tin-polydimethylsiloxane composites. Pure Appl Chem. 2025. https://doi.org/10.1515/pac-2024-0347.
40. Knoll GF. Radiation Detection and Measurement. 4th ed. Hoboken (NJ): John Wiley & Sons; 2010.
41. Bijanu A, Arya R, Agrawal V, Tomar AS, Gowri VS, Sanghi SK, *et al.* Metal-polymer composites for radiation protection: a review. J Polym Res. 2021. https://doi.org/10.1007/s10965-021-02751-3.
42. McCaffrey JP, Tessier F, Shen H. Radiation shielding materials and radiation scatter effects for interventional radiology (IR) physicians. Med Phys. 2012;39(7):4537–4546. https://doi.org/10.1118/1.4730504.
43. Jayakumar S, Saravanan T, Philip J. A review on polymer nanocomposites as lead-free materials for diagnostic X-ray shielding: Recent advances, challenges and future perspectives. Hybrid Adv. 2023;4:100100. https://doi.org/10.1016/j.hybadv.2023.100100.
44. Rueden CT, Schindelin J, Hiner MC, DeZonia BE, Walter AE, Arena ET, *et al.* ImageJ2: ImageJ for the next generation of scientific image data. BMC Bioinformatics. 2017;18(1). https://doi.org/10.1186/s12859-017-1934-z.
45. Alresheedi MT, Elsafi M, Aladadi YT, Abas AF, Ganam A, Sayyed MI, *et al.* Assessment of silicone rubber/lead oxide composites. Polymers (Basel). 2023;15(9). https://doi.org/10.3390/polym15092160. .
46. Almurayshid M, Alssalim Y, Aksouh F, Almsalam R, Alqahtani M, Sayyed MI, *et al.* Development of new lead-free composite materials as potential radiation shields. Materials. 2021;14(17):1–10. https://doi.org/10.3390/ma14174957.
47. ÖzkalaycıF, Kaçal MR, Agar O, Polat H, Sharma A, Akman F. Lead(II) chloride effects on nuclear shielding capabilities of polymer composites. J Phys Chem Solids. 2020;145:109543. https://doi.org/10.1016/j.jpcs.2020.109543.
48. Li Z, Zhou W, Zhang X, Gao Y, Guo S. High-efficiency, flexibility and lead-free X-ray shielding multilayered polymer composites: layered structure design and shielding mechanism. Sci Rep. 2021;11(1):1–13. https://doi.org/10.1038/s41598-021-83031-4.
49. Pianpanit T, Saenboonruang K. High-energy photon attenuation properties of lead-free and self-healing poly(vinyl alcohol) (PVA) hydrogels: numerical determination and simulation. Gels. 2022;8(4). https://doi.org/10.3390/gels8040197.
50. Chang L, Zhang Y, Liu Y, Fang J, Luan W, Yang X, *et al.* Preparation and characterization of tungsten/epoxy composites for γ-rays radiation shielding. Nucl Instrum Methods Phys Res B. 2015;356–357:88–93. https://doi.org/10.1016/j.nimb.2015.04.062.
51. Alshahri S, Alsuhybani M, Alosime E, Alotaibi S, Almurayshid M, Alrwais A. LDPE/bismuth oxide nanocomposite: Preparation, characterization and application in x-ray shielding. Polymers (Basel). 2021;13(18). https://doi.org/10.3390/polym13183081.
52. Oglat AA. Studying the radiation absorption and scattering of gamma rays by using different absorbers. Radiat Phys Chem. 2020;176:109072. https://doi.org/10.1016/j.radphyschem.2020.109072.
53. Abdalsalam AH, Sayyed MI, Ali Hussein T, Şakar E, Mhareb MHA, Ceviz Şakar B, *et al.* A study of gamma attenuation property of UHMWPE/Bi_2O_3 nanocomposites. Chem Phys. 2019;523:92–98. https://doi.org/10.1016/j.chemphys.2019.04.013.
54. Zainal Abidin H, Mukhtar NMA, Mahmood A, Abdul Wahab NA, Zainon R, Roslan NS, *et al.* Radiation shielding properties of tin-polydimethylsiloxane (PDMS) composites against gamma ray at 356 keV. Int J Innov Ind Rev. 2025;7(20):352–369. https://doi.org/10.35631/IJIREV.720023.
55. Ramli M, Tabassi AA, Hoe KW. Porosity, pore structure and water absorption of polymer-modified mortars: An experimental study under different curing conditions. Compos B Eng. 2013;55:221–233. https://doi.org/10.1016/j.compositesb.2013.06.022.
56. Medhat ME, Singh VP. Mass attenuation coefficients of composite materials by Geant4, XCOM and experimental data: comparative study. Radiat Eff Defects Solids. 2014; 169(9):800–807. https://doi.org/10.1080/10420150.2014.950264.

المسامية والسلامة الهيكلية لمركبات القصدير ثنائي ميثيل سيلوكسان (PDMS)لتطبيق الحماية من الإشعاع

هانيسة زين العابدين[1]، نور ميزة العزرة مختار[1،2،3]، عينوركيلا محمود[1]، نور ايمي عبد الوهاب[1]، رفيدة زينون[3]، نور شفيقة رسلان[1]، نور إيواني نور إزاحام[4]، عائشة زرزالي شاه[5]

[1]قسم العلوم التطبيقية، جامعة التكنولوجيا مارا، كاوانجان، بولاو بينانج، 13500 بيرماتانج باوه، بولاو بينانج، ماليزيا.
[2]كلية العلوم الصحية، جامعة التكنولوجيا مارا كاوانجان بولاو بينانج، 13200 كيبالا باتاس، بولاو بينانج، ماليزيا.
[3]قسم التصوير الطبي الحيوي، المعهد المتقدم للطب وطب الأسنان، جامعة سينز الماليزية، *SAINS@BERTAM*، 13200 كيبالا باتاس، بولاو بينانج، ماليزيا.
[4]كلية العلوم التطبيقية، جامعة التكنولوجيا مارا ، 40450 شاه علم، سيلانجور، ماليزيا.
[5]مركز الدراسات التأسيسية*UiTM* ، جامعة التكنولوجيا مارا كاوانجان سيلانجور، كامبوس دينجكيل، 43800 دينجكيل، سيلانجور، ماليزيا.

الملخص

تُعَدّ الإشعاعات المؤيّنة مفيدة في العلاجات والتشخيصات الطبية، إلا أنها تُشكِّل في الوقت ذاته مخاطر صحية كبيرة، مثل الإشعاع المتناثر والتعرّض غير المقصود. ويُعَدّ الرصاص من أكثر المواد استخداماً في الحماية الإشعاعية لما يتمتع به من قدرة عالية على إضعاف أشعة غاما، لكنه يسبب تحديات بيئية وهندسية. يهدف هذا البحث إلى تقييم الخصائص التركيبية وإمكانات الامتصاص الإشعاعي لمتراكبات القصدير–البولي دايميثيل سيلوكسان .(PDMS) جرى تصنيع المتراكبات بتراكيز معدنية مختلفة واختبارها من حيث كفاءة الحماية من الإشعاع(RPE) ، والخصائص التركيبية، والبنية الكيميائية، والمساميّة. كما استُخدم مطياف أشعة غاما لتحليل الإشعاع، مع استخدام Cd-109 كمصدر رئيسي. أظهر متراكب القصدير النقي (PT) PDMS/أعلى كفاءة في الحماية الإشعاعية مقارنة بمتراكب سبيكة النحاس–القصدير (TA) PDMS/ومتراكب سبيكة النحاس–القصدير مع القصدير النقي(PA) PDMS/، ويُعزى ذلك إلى العدد الذري المرتفع للقصدير وانخفاض المسامية فيه. وقد أكدت الفحوصات التركيبية والكيميائية، بما في ذلك تحليل FESEM وFTIR، تجانس المتراكبات وروابطها الكيميائية. وتمّ تقييم مسامية المتراكبات باستخدام برنامجImageJ ، حيث أظهرت النتائج ازدياد المسامية مع زيادة نسبة الحشو المعدني في المتراكبات. ومع ذلك، فإن قدرة التوهين الإشعاعي تأثرت بشكل أكبر بالعدد الذري للمعدن المستخدم ونسبة الحشو المعدني داخل المتراكبات. أظهرت تحليلات المسامية أن متراكب PT يمتلك أقل مسامية بين العينات، مما قد يُسهم في كفاءته الأعلى في الحماية الإشعاعية. وعلى النقيض، أظهر كل من TA و PAانخفاضاً في العدد الذري وارتفاعاً في المسامية، مما أضعف سلامتهما الهيكلية وقد يقلل من قدرتهما على توهين الفوتونات. وعليه، تُقترح تقنيات مثل الضغط الحراري، وإزالة الغازات، أو التفريغ لتحسين تقليل المسامية وتعزيز كفاءة الحماية الإشعاعية في هذه المتراكبات.

الكلمات المفتاحية: المركبات، المعدن، البوليمر، المسامية، الحماية الإشعاعية.